nature chemistry

ARTICLES

PUBLISHED ONLINE: 10 MARCH 2013 | DOI: 10.1038/NCHEM.1596

Synthesis of 19-substituted geldanamycins with altered conformations and their binding to heat shock protein Hsp90

Russell R. A. Kitson[1], Chuan-Hsin Chang[2], Rui Xiong[2], Huw E. L. Williams[1], Adrienne L. Davis[1], William Lewis[1], Donna L. Dehn[2], David Siegel[2], S. Mark Roe[3], Chrisostomos Prodromou[3]*, David Ross[2]* and Christopher J. Moody[1]*

The benzoquinone ansamycin geldanamycin and its derivatives are inhibitors of heat shock protein Hsp90, an emerging target for novel therapeutic agents both in cancer and in neurodegeneration. However, the toxicity of these compounds to normal cells has been ascribed to reaction with thiol nucleophiles at the quinone 19-position. We reasoned that blocking this position would ameliorate toxicity, and that it might also enforce a favourable conformational switch of the *trans*-amide group into the *cis*-form required for protein binding. Here, we report an efficient synthesis of such 19-substituted compounds and realization of our hypotheses. Protein crystallography established that the new compounds bind to Hsp90 with, as expected, a *cis*-amide conformation. Studies on Hsp90 inhibition in cells demonstrated the molecular signature of Hsp90 inhibitors: decreases in client proteins with compensatory increases in other heat shock proteins in both human breast cancer and dopaminergic neural cells, demonstrating their potential for use in the therapy of cancer or neurodegenerative diseases.

Heat shock protein 90 (Hsp90) is one of the most abundant proteins in eukaryotic cells and, driven by the hydrolysis of adenosine tri-phosphate (ATP), is a molecular chaperone responsible for the folding of nascent proteins. It has been described as the master regulator of the stabilization, activation and degradation of a range of over-expressed or mutant oncogenic proteins[1]. Its inhibition can cause client proteins to adopt misfolded conformations that are ubiquinated and subject to proteasomal degradation, thereby simultaneously disrupting multiple cancer-causing pathways. As a consequence, it has emerged as a very attractive target for novel molecular cancer therapeutic agents[2–6], and there are now more than 15 Hsp90 inhibitors in clinical trials, with accumulating evidence of anticancer activity[3,6,7]. In addition, the modulation of protein folding is also relevant to neurodegenerative diseases, and a number of conditions such as Alzheimer's and Parkinson's diseases are thought to be associated with protein misfolding and aggregation[8–14].

One compound that has played a very major role in the Hsp90 arena is the benzoquinone ansamycin (BQA) geldanamycin. However, its use is limited because of the hepatotoxicity observed in preclinical studies[15], possibly a result of reaction with biological nucleophiles at the reactive 19-position of the quinone ring[16–18]. We reasoned that blocking the reactive 19-position might suppress this reaction with biological nucleophiles, ameliorate toxicity, and also result in a conformational change arising from amide *trans* to *cis* isomerism. We now report the realization of this hypothesis. Introducing a substituent at C19 does indeed cause the desired conformational switch, while also blocking reaction with thiol nucleophiles and, importantly, markedly reducing toxicity to normal endothelial and epithelial cells. Additionally, studies in both human breast cancer cells and dopaminergic neural cells established that the novel 19-substituted BQAs are effective inhibitors of Hsp90, suggesting that such rationally modified compounds have potential for application in the therapy of cancer and neurodegenerative diseases.

Geldanamycin **1**, a naturally occurring BQA polyketide, is a potent inhibitor of Hsp90, and its binding to the *N*-terminal domain has been studied by X-ray crystallography[19,20] and NMR spectroscopy[21]. In preclinical studies, geldanamycin was found to exhibit significant hepatotoxicity[15], so other less toxic and more soluble benzoquinone ansamycins such as 17-allylamino-17-demethoxygeldanamycin (17-AAG, tanespimycin) **2** and 17-(2-dimethylaminoethylamino)-17-demethoxygeldanamycin (17-DMAG, alvespimycin) **3** were developed. Although 17-AAG (tanespimycin) **2** showed some promise in Phase II trials, demonstrating activity in HER2/ERBB2-positive trastuzumab-refractory breast cancer[22], development of the compound has been halted, further emphasizing the need for less toxic derivatives.

In neuroscience, protein misfolding can be regulated by chaperones such as Hsp70, which paradoxically can be induced by inhibition of Hsp90. The chaperones Hsp90 and 70 exhibit very different specificity with respect to client protein interactions, providing a mechanism whereby inhibiting one chaperone (Hsp90) while inducing another (Hsp70) can be beneficial in specific diseases. Hence, Hsp90 has now emerged as a target to prevent neurodegeneration[8–14], and Hsp90 inhibitors have been used as protective therapies in mouse models of Parkinson's disease[23]. The BQAs geldanamycin and 17-AAG have been found to protect against 1-methyl-4-phenyl-1,2,3,6-tetrahydropyridine (MPTP)-induced dopaminergic neurotoxicity in mice[23], and other models of neurodegenerative disease[9,24–26].

However, if such BQAs are to be considered as potential therapeutic agents for neurodegenerative disease, there is an urgent

[1]School of Chemistry, University of Nottingham, University Park, Nottingham NG7 2RD, UK, [2]Department of Pharmaceutical Sciences, School of Pharmacy, University of Colorado Denver, 12700 East 19th Avenue, Aurora, Colorado 80045, USA, [3]Genome Damage and Stability Centre, Science Park Road, University of Sussex, Falmer, Brighton BN1 9RQ, UK. *e-mail: chris.prodromou@sussex.ac.uk; c.j.moody@nottingham.ac.uk; david.ross@ucdenver.edu

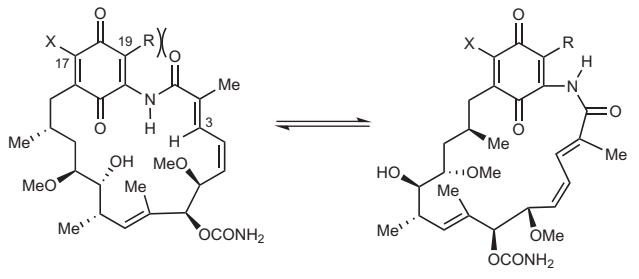

Figure 1 | *Trans–cis* amide isomerization in geldanamycin BQAs. Does the steric strain caused by introduction of a substituent R at the 19-position enforce a favourable conformational switch of the *trans*-amide group into the *cis*-form required for protein binding, while also ameliorating toxicity by blocking attack of biological nucleophiles?

need to reduce their toxicity while retaining or improving their potency. The toxicity has been proposed to arise from the reaction of biological nucleophiles, particularly glutathione, at the unsubstituted 19-position of the quinone ansamycin[16–18]. We reasoned that the conjugation of glutathione (or other nucleophiles) might be suppressed by blocking the 19-position of the BQAs, and, as a result, the toxicity issues might be ameliorated. In addition, we also hypothesized that the introduction of a substituent at C19 would result in conformational changes in the macrocyclic ring, arising from the 19-substituent causing amide *trans* to *cis* isomerism as a result of steric strain. We now report the first studies on the design and synthesis of a range of such 19-substituted BQAs, a study of their conformation in solution by NMR spectroscopy, their binding to yeast Hsp90 by protein X-ray crystallography, their reaction with thiol nucleophiles, and studies on toxicity and Hsp90 inhibition in cellular systems.

Results and discussion

Compound design and rationale. The BQA macrocycles are known to adopt an extended *trans*-amide conformation in the solid state, as shown by X-ray crystal structures of geldanamycin **1** itself[27] and the 17-azetidinyl compound **4** (ref. 28). Early NMR spectroscopic studies on the solution conformation of BQA **4** also suggested a *trans*-amide conformation on the basis of the strong nuclear Overhauser effect (nOe) enhancement between the NH and the alkene H-3 (Fig. 1)[28]. In contrast, protein crystallography studies using either yeast or human Hsp90 have shown that, on binding, geldanamycin **1** and 17-DMAG **3** adopt a more closed 'C-clamp' conformation with a *cis*-amide bond[19,20,29], so the isomerization equilibrium (Fig. 1) between *trans* and *cis* forms is a matter of some debate. Although some computational studies have put the barrier to *trans–cis* isomerization as >80 kJ mol^{-1} (ref. 30), other calculations suggest that it is much lower than this[31]. A requirement for *trans–cis* isomerization of the BQA for binding and inhibition of Hsp90 has been suggested[29,30], but a separate study has disputed this conclusion[32,33]. We therefore set out to synthesize a wide range of stable geldanamycin analogues, containing diverse substituents at the 19-position, to investigate both the toxicological implications and also whether any conformational 'switch' was observed.

Synthesis. Geldanamycin and related BQAs such as the herbimycins and macbecins have been the subject of a number of studies, ranging from total synthesis of the natural products themselves to their synthetic modification[34,35]. A small number of 19-substituted geldanamycin derivatives have been prepared previously by modification of the natural product, either by exploiting the nucleophilic character of the amino-quinone moiety (for example, halogenation[36] and Mannich[37,38] reactions) or the ability of the quinone to act as a conjugate acceptor by reacting with nucleophiles such as thiols[39], amines[26,37] and alcohols[26,40]. Given the limited applicability of the aforementioned methods, particularly for the formation of a C–C bond at the 19-position, we were attracted to the possibility of utilizing a palladium-catalysed cross-coupling. Such protocols, including the Heck, Suzuki, Stille, Negishi and Sonagashira reactions, constitute a versatile and powerful strategy in modern chemistry, and have the advantage that a wide array of coupling partners are readily available, allowing access to a diverse set of 19-substituted analogues.

To assess the viability of the cross-coupling approach, we commenced with the stable and readily accessible 19-iodogeldanamycin **5**, prepared in excellent yield via the remarkably selective reaction of commercially available geldanamycin **1** with iodine (Fig. 2a)[36]. Unfortunately, difficulties were immediately encountered using standard conditions for cross-couplings with a range of partners (boronic acids or boronate esters, stannanes, Grignards, alkynes and alkenes) and different metal catalysts (predominantly palladium and iron), with the sensitivity of the different functionalities within the BQA substrate proving incompatible with many conditions (high temperature and strong base). In addition, couplings under milder conditions (those at lower temperature or with mild or no base) also proved to be problematic, with only the formation of geldanamycin itself observed, presumably due to competing reductive catalytic processes. We hypothesized that these findings may be due to the transmetallation step in the catalytic cycle being slower than that for a competing pathway. Thus, we subjected our substrate to modified conditions that have been reported to address such problems, focusing on the Stille reaction, as this is generally considered the mildest of palladium-catalysed cross-coupling processes.

The replacement of phosphine ligands with triphenylarsine has been well documented to assist slow transmetallations[41], the softer and more labile arsine ligand facilitating the formation of the palladium–tin double-bond π-complex, which has been reported to be the rate-determining step in Stille cross-couplings[42]. We were delighted to observe that performing the Stille coupling with tetramethyltin in the presence of triphenylarsine gave 19-methylgeldanamycin **6**, albeit in moderate yield and with significant quantities of recovered geldanamycin (29%). Following this promising result, a range of optimization reactions were carried out (Supplementary Table S2), resulting in the establishment of optimal conditions of 1.2 equiv. stannane, 20 mol% arsine, 5 mol% $Pd_2(dba)_3{\cdot}CHCl_3$ and 5 mol% CuI (ref. 43) in *N*,*N*-dimethylformamide (DMF) at 35 °C. This gave the desired 19-substituted BQA **6** in an excellent yield of 86%.

Having established a successful coupling protocol, we investigated the scope of the reaction with a range of stannane coupling partners, selected to introduce representative alkyl, alkenyl, aryl and hetaryl groups (Fig. 2a). Although a methyl group could be successfully incorporated at C19, attempted coupling of other alkyl groups was unsuccessful. Similarly, the reaction of 19-iodogeldamycin **5** with allyl tri-*n*-butylstannane only gave a very poor yield (~5%) of the 19-allyl compound. Both electron-rich and electron-deficient aromatic groups could also be coupled successfully in good to excellent yield. Heteroaromatic stannanes proved to be more variable under our conditions. Coupling of the 2-pyridyl group was problematic, with the product **12** isolated in a moderate yield of 30%. However, furan and thiophene groups were successfully transferred, affording substrates **13** and **14** in excellent yields of 90% and 94%, respectively. The Stille products, following an aqueous work-up and purification (K_2CO_3/SiO_2 chromatography)[44],

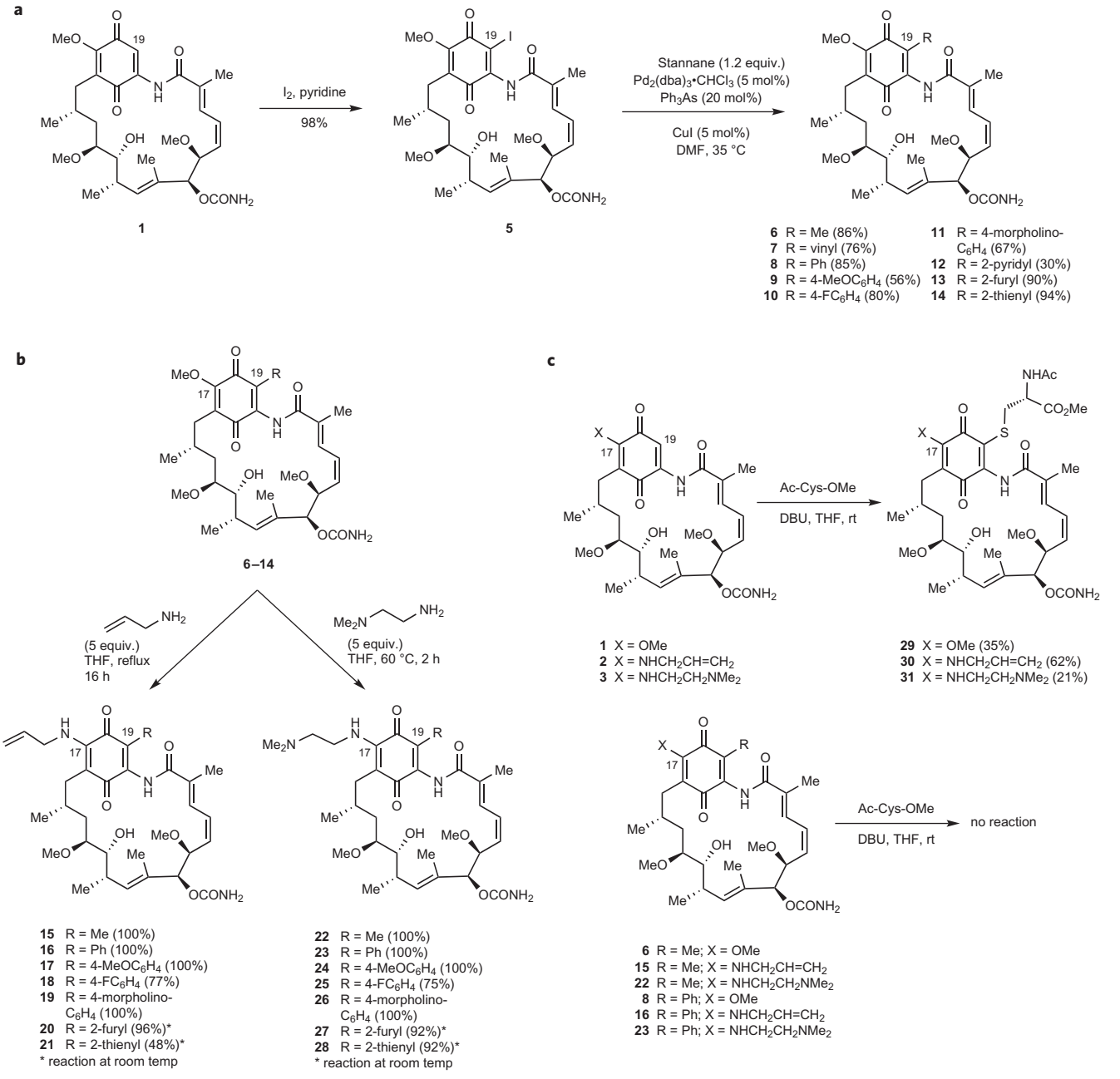

Figure 2 | Synthesis and reactivity of 19-substituted geldanamycin derivatives. a, Synthesis of 19-substituted geldanamycins by selective iodination and optimized palladium-catalysed Stille coupling. **b**, Synthesis of 17-allylamino- and 17-(2-dimethylaminoethylamino)-19-substituted geldanamycins (**15–21** and **22–28**, respectively) by displacement of the 17-methoxy group with amines. **c**, Addition of *N*-acetylcysteine methyl ester to BQAs **1–3**, with formation of the corresponding 19-substituted adducts **29–31**. The 19-substituent in the methyl (**6**, **15**, **22**) and phenyl (**8**, **16**, **23**) compounds prevents similar nucleophilic attack of the *N*-acetylcysteine methyl ester. dba, dibenzylideneacetone; DBU, 1,8-diazabicyclo[5.4.0]undec-7-ene.

contained 10.5 ppm palladium, 7.9 ppm tin and arsenic, and undetectable levels of copper, as detected by inductively coupled plasma mass spectrometry (ICPMS) trace element analyses (for details, see Supplementary Section, 'ICPMS trace element analysis', page S52).

In the geldanamycin series of BQAs, it is the 17-allylamino (17-AAG) and 17-(2-dimethylaminoethylamino) (17-DMAG) derivatives **2** and **3** that have shown the most clinical promise, so we synthesized the corresponding AAG and DMAG analogues of our 19-substituted geldanamycin derivatives (Fig. 2b). This was readily achieved by heating the 17-methoxy compounds **6–14** with a fivefold excess of allylamine or *N*,*N*-dimethylethylenediamine in tetrahydrofuran (THF), and gave the corresponding 17-amino derivatives in modest to excellent yield. In the main, the substitutions proceeded smoothly, although the 19-vinyl derivative **7** gave no product, presumably due to competing conjugate addition reactions.

Conformational studies. Interestingly, the 19-substituted derivatives **6–14** were significantly more polar than geldanamycin itself (silica gel TLC $R_f = 0.29$ (where R_f is retardation factor) (19-methylgeldanamycin) versus 0.56 (geldanamycin) in 2:1 ethyl acetate/light petroleum). To investigate whether this was as a result of the proposed conformational 'switch', we undertook a series of detailed NMR spectroscopic experiments. Conformational NMR studies of geldanamycin **1** and 17-azetidinyl-17-demethoxygeldanamycin **4**

have been reported previously. For amino derivative 4, qualitative nOe analysis of the compound was consistent with the *trans*-amide conformation[28]. Quantitative rotating-frame nuclear Overhauser effect correlation spectroscopy (ROESY) experiments performed on geldanamycin 1 itself gave calculated inter-atomic distances that were again consistent with an extended conformation and a *trans*-configured amide[31].

The NMR chemical shift data obtained in our work immediately suggested conformational disparities between geldanamycin 1 and our synthesized derivatives, with all of the 19-substituted compounds exhibiting ^{1}H chemical shift patterns that were significantly different from those of the parent molecule. These differences in the NMR spectra (Supplementary Figs S3 and S4) indicate a major change in the environment of many of the positions, both those influenced by a potential change in the amide configuration, and also those in the opposite section of the macrocycle, reinforcing the evidence for a change in the conformation of the ansa ring. The ^{13}C shifts, being relatively unaffected by the magnetic anisotropy of other atoms or groups (unlike ^{1}H, for example, aromatic ring currents), are particularly compelling in this regard. We also investigated the through-space correlations detected in nuclear Overhauser effect correlation spectroscopy (NOESY) and ROESY spectra, as well as undertaking a quantitative nOe study of 19-phenyl-AAG 16, with subsequent molecular modelling investigations. These studies (for details, see Supplementary pages S57–S75) strongly suggest that the dominant form in solution is a *cis*-amide adopting a C-clamp type conformation. From the model, it is clear that the compact C-shaped conformation allows the hydrophobic surface area to be minimized by being 'buried' in the heart of the structure, while the hydrophilic moieties are exposed to the solvent. This observation would be consistent with the large difference in polarity observed by thin layer chromatography (TLC) analysis.

To confirm that 19-substitution caused a *trans* to *cis* amide change in conformation in the solid state, we sought evidence from X-ray crystallography. 19-(2-Furyl)geldanamycin 13 gave crystals (of its THF complex) that were suitable for X-ray diffraction. The molecule exhibited both the *cis*-configured amide and also the 'C-clamp' conformation (Supplementary Fig. S12; CCDC reference 864025). Unsurprisingly, therefore, the conformation of macrocycle 13 is different to that of 19-unsubstituted geldanamycins that adopt a *trans*-amide conformation in the crystal; this is clearly seen by overlaying the structure of 13 and the published structure of compound 4 (ref. 28), as depicted in Fig. 3a. On the other hand, and in line with our original hypothesis, the isomerization from *trans*- to *cis*-amide induced by the 19-substituent does impart an overall 'C-clamp' conformation to the BQA macrocycle that is very similar to that of the protein-bound geldanamycin, as shown in the overlaid structures in Fig. 3b.

Substitution at C19 prevents nucleophilic attack. Part of the rationale for the incorporation of a substituent at the 19-position was that it would block the potential for metabolism by nucleophilic attack of glutathione[16–18], and hence might ameliorate the quinone-related hepatotoxicity seen with BQAs. We therefore tested whether our 19-substituted analogues would react with thiol nucleophiles. *N*-Acetylcysteine methyl ester was utilized as a model for glutathione and was initially introduced to geldanamycin 1, 17-AAG 2 and 17-DMAG 3 under neutral conditions. Although this resulted in no reaction, basic conditions (1,8-diazabicyclo[5.4.0]undec-7-ene (DBU), THF, room temperature) afforded the corresponding adducts 29–31 in 35%, 62% and 21% unoptimized yields, respectively (Fig. 2c). On subjecting our 19-methyl and 19-phenylgeldanamycin derivatives to identical conditions, no reaction was observed with the thiol at C19, even upon heating of the reaction mixture.

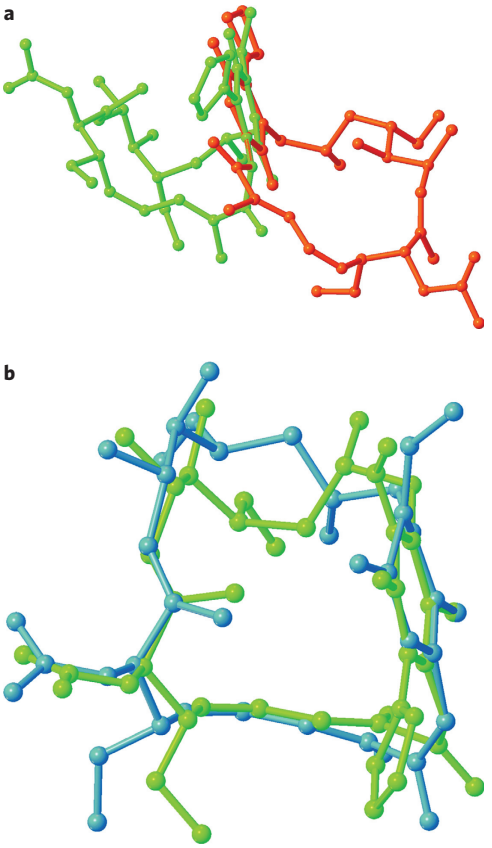

Figure 3 | Overlaid crystal structures reveal the effect of 19-substitution on geldanamycin conformation and binding. a, The different conformations of 19-(2-furyl)geldanamycin 13 (green) with a *cis*-amide and 19-unsubstituted-17-azetidinylgeldanamycin 4 (orange) with a *trans*-amide[28]. **b**, Similarity between the unbound *cis*-amide conformation of 19-(2-furyl)geldanamycin 13 (green) and protein-bound geldanamycin 1 (blue) from the yeast Hsp90–geldanamycin complex[20].

Substitution at C19 reduces toxicity in cells. A key tenet of our original hypothesis was that introduction of a substituent at C19 would not only cause the desired conformational switch, but would also prevent nucleophilic attack by thiols, thereby ameliorating the toxicity of the parent BQAs. With the first two features now established, we sought evidence for reduced toxicity, and therefore evaluated the toxicity of the 19-substituted compounds in comparison to their parent BQAs in reducing toxicity in normal endothelial and epithelial cellular systems. We

Table 1 | Toxicity of benzoquinone ansamycins.

Compound	HUVECs* IC_{50} (μM)	ARPE-19 IC_{50} (μM)
Geldanamycin 1	0.041±0.003	0.10±0.04
19-Me-geldanamycin 6	16.9±3.3	>20
19-Ph-geldanamycin 8	2.1±0.4	8.3±0.7
17-AAG 2	1.2±0.1	1.0±0.4
19-Me-17-AAG 15	>20	>20
19-Ph-17-AAG 16	>20	>20
17-DMAG 3	0.88±0.04	0.15±0.01
19-Me-17-DMAG 22	>20	>20
19-Ph-17-DMAG 23	17.7±1.6	8.2±0.4

*HUVEC are primary cells and ARPE-19 cells are a non-transformed human retinal pigmented epithelial cell line. Toxicity values were generated using the 3-(4,5-dimethylthiazol-2-yl)-2,5-diphenyltetrazolium bromide (MTT) assay. The values are represented as a mean±standard deviation ($n=3$). IC_{50} (half-maximal inhibitory concentration) of 19-substituted BQAs and their parent quinones. Culture conditions and the MTT assay are described in Supplementary section, 'Toxicity Studies: Methods', page S82.

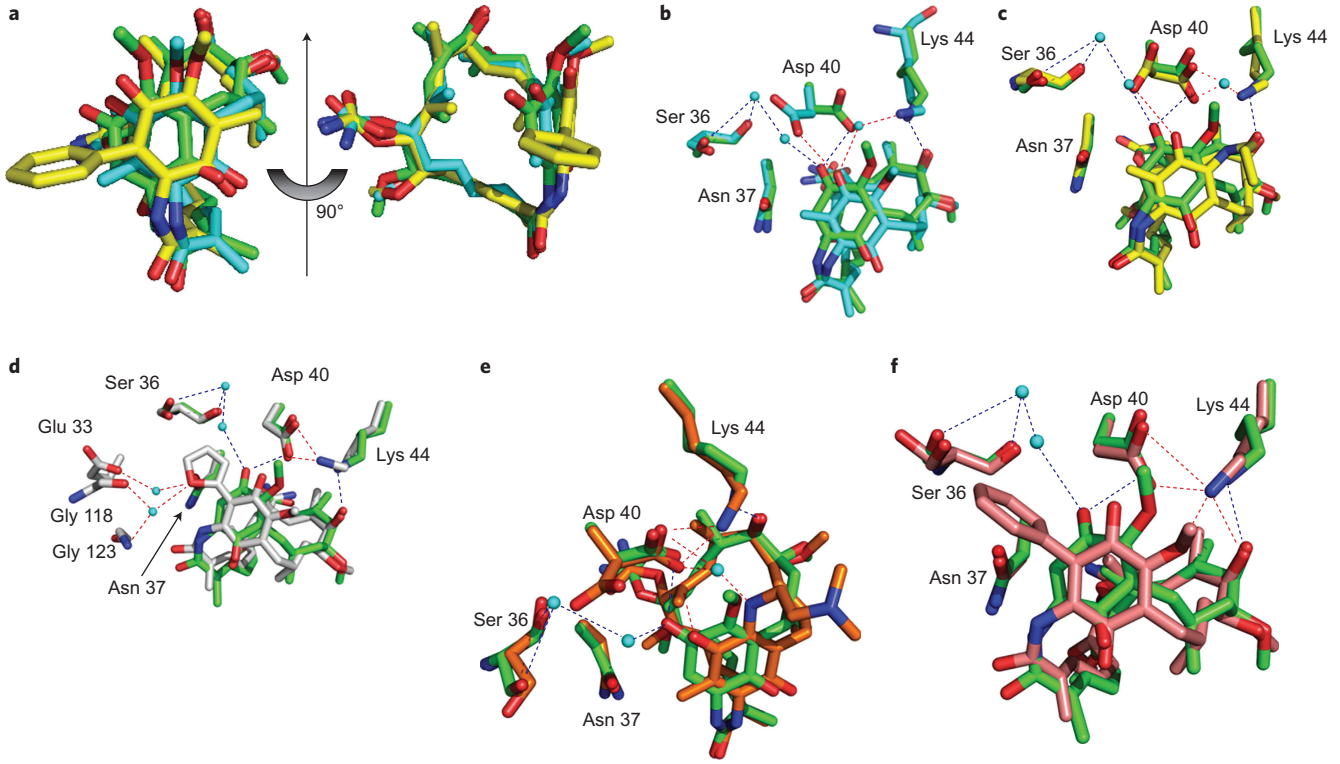

Figure 4 | Structures of 19-substituted geldanamycins bound in the ATP site of yeast Hsp90, as determined by protein X-ray crystallography. a, Two orthogonal views of the superimposition of geldanamycin **1** (green), 19-methyl geldanamycin **6** (cyan) and 19-phenyl geldanamycin **8** (yellow), from the co-crystal structures of *N*-terminal yeast Hsp90, showing the similarity of the bound conformations. **b**–**f**, Comparison of the binding of geldanamycin with 19-substituted geldanamycin analogues to the *N*-terminal domain of yeast Hsp90. PyMol diagrams showing the interactions of geldanamycin **1** (green) and 19-methyl geldanamycin **6** (cyan) with Hsp90 (green and cyan residues, respectively (**b**); geldanamycin **1** (green) and 19-methyl 17-AAG **15** (yellow) with Hsp90 (green and yellow residues, respectively) (**c**); geldanamycin **1** (green) and 19-(2-furyl) geldanamycin **13** (grey) with Hsp90 (green and grey residues, respectively) (**d**); geldanamycin **1** (green) and 19-methyl 17-DMAG **22** (gold) with Hsp90 (green and gold residues, respectively) (**e**); geldanamycin **1** (green) and 19-phenyl geldanamycin **8** (salmon) with Hsp90 (green and salmon residues, respectively) (**f**). In general, in these geldanamycin analogues, the 19-substituents tend to alter binding to the protein through a positional change of the quinone group of the benzoquinone ansamycin. Dotted blue lines, hydrogen bonds involving geldanamycin; dotted red lines, hydrogen bonds involving 19-substituted analogues; cyan-coloured spheres, water molecules. The structures for geldanamycin and the 19-substituted derivatives were obtained at 2.0 Å (geldanamycin), 2.7 Å (19-methyl geldanamycin), 2.25 Å (19-methyl 17-AAG), 3.1 Å (19-methyl 17-DMAG), 2.2 Å (19-phenyl geldanamycin) and 2.6 Å (19-(2-furyl) geldanamycin) resolutions. For atomic coordinates and structure factors, see PDB codes 1A4H, 4AS9, 4ASA, 4ASB, 4ASG and 4ASF, respectively.

used human umbilical vein endothelial cells (HUVECs) and retinal pigmented epithelial cells (ARPE-19 cells) in these studies. Our data (Table 1) clearly demonstrate that 19-substitution markedly reduces BQA toxicity in all series of compounds tested. Both 19-methyl and 19-phenyl BQAs in the geldanamycin, 17-AAG and 17-DMAG series were markedly less toxic than their parent quinones.

Binding to Hsp90. We analysed the thermodynamics of the binding of 19-methylgeldanamycin to the *N*-terminal domain of yeast Hsp90 using isothermal titration calorimetry (ITC). Geldanamycin binds to the protein with ~1:1 stoichiometry with a K_d of 2.9 μM. The binding is accompanied by a favourable enthalpy change, although it does incur an entropic penalty. For the 19-methyl derivative **6**, there is an approximately fivefold loss of binding affinity ($K_d = 16.3$ μM) relative to geldanamycin itself, with a loss of enthalpic contribution, somewhat compensated for by an increase in entropic contribution favouring binding. To investigate the reasons for this slight loss of binding upon introduction of the 19-methyl group, we turned to protein X-ray crystallography.

The crystal structure of geldanamycin with the *N*-terminal domain of yeast Hsp90 has been determined previously[20], so we studied the Hsp90 complexes of the 19-substituted geldanamycins for comparison. Geldanamycin and its 19-substituted derivatives essentially bind in the same way to the *N*-terminal domain of Hsp90 (Fig. 4a), with, as expected, a *cis*-amide conformation. However, all the 19-substituted analogues show a shift in the position of the quinone ring (Fig. 4b–f) relative to the geldanamycin complex to avoid a steric clash with Asn 37, consequently altering some of the interactions in these complexes relative to the geldanamycin–Hsp90 complex. For example, in the geldanamycin–Hsp90 complex, Lys 44 is normally hydrogen-bonded to the 13-hydroxy group of geldanamycin. With 19-methyl geldanamycin **6**, the repositioning of the quinone group results in Lys 44 forming a hydrogen bond, via a water molecule, with one of the quinone oxygens of 19-methyl geldanamycin (Fig. 4b). For geldanamycin, the same quinone oxygen normally forms a hydrogen bond with one of the oxygens of Asp 40, while in the 19-methyl geldanamycin–Hsp90 complex, Asp 40 adopts an alternative conformation that disrupts a pre-existing network of water-mediated hydrogen bonds between the same quinone group in question and the hydroxyl oxygen and main-chain oxygen of Ser 36 (Fig. 4b). Loss of these waters might account for the increase in the entropic contribution favouring binding. A similar effect is also seen with the 19-methyl derivative of 17-DMAG **22** (Fig. 4e). With 19-methyl 17-AAG **15** and 19-methyl 17-DMAG **22** we see essentially the same changes,

except that the Asp 40 residue appears to flip between the two alternative conformations seen. Consequently, 19-methyl 17-AAG **15** makes hydrogen bonds (via water molecules) to Lys 44, but the quinone oxygen interactions (via two water molecules) with Ser 36 appear disrupted (Fig. 4c). Similarly, for 19-methyl 17-DMAG **22**, Lys 44 forms direct hydrogen bonds with Asp 40, while another hydrogen bond (via a water molecule) is seen between one of the Asp 40 oxygens and the amide nitrogen of the 17-DMAG group (Fig. 4e). For 19-phenyl **8** and 19-(2-furyl)-geldanamycin **13**, the Asp 40 adopts its geldanamycin bound conformation. However, for these compounds, Lys 44 forms two direct hydrogen bonds with the side-chain oxygens of Asp 40 (Fig. 4d,f). For the 19-(2-furyl) analogue **13**, we also see some additional hydrogen-bond interaction with the 2-furyl group oxygen. This oxygen atom forms a network of hydrogen bonds (via water molecules) to the main-chain amide of Gly 123, the main-chain carbonyl of Gly 118 and to one of the oxygens of the catalytic Glu 33 residue (Fig. 4d). However, collectively, the results indicate that in these geldanamycin analogues, the 19-substituents tend to alter binding to the protein through forced positional change of the quinone group of the benzoquinone ansamycin. This is in spite of the fact that these 19-substituted compounds already exist in the *cis*-amide conformation required for binding to Hsp90, as can be seen for the 19-(2-furyl) analogue **13**, where the protein bound conformation is very similar, although not completely identical, to that seen in the crystal structure of this analogue alone (Fig. 3; Supplementary Fig. S12).

Inhibition of Hsp90 in cellular systems. X-ray crystallography clearly showed that 19-substituted derivatives do bind to the ATP site in Hsp90. We therefore examined the ability of 19-substituted compounds to inhibit Hsp90 in cellular systems. A decrease in Hsp90 client proteins (including Raf1, Her2 and Cdc-2) and a compensatory increase in Hsp70 are the two most common biomarkers used for inhibition of Hsp90 in cells[45–47]. Initially, we used MDA-468-NQ16 cells that over-express the quinone reductase NQO1, because we have shown that NQO1 potentiates Hsp90 inhibition due to the formation of the more active hydroquinone ansamycin[45,46], and worked with the 17-DMAG (alvespimycin) series. In Fig. 5a we demonstrate that both 17-DMAG and 19-phenyl 17-DMAG are effective Hsp90 inhibitors, as shown by decreases in Hsp90 client proteins and compensatory induction of Hsp70. We extended these data to the Her2-positive BT474 breast cancer cell line, and both DMAG and 19-phenyl DMAG resulted in degradation of Hsp90 clients, including Her2, as well as inducing a compensatory increase in Hsp70 (Fig. 5b).

In addition to their use as anticancer agents, Hsp90 inhibitors have attracted attention as potential protective agents against neurodegeneration due to their ability to induce a compensatory increase in other heat shock proteins that protect against aberrant protein folding and aggregation[8–14]. SH-SY5Y neuroblastoma cells are dopaminergic and have been used as a cellular model system of relevance to Parkinson's disease[48–50]. In Fig. 5c, we demonstrate that both geldanamycin and 19-phenyl geldanamycin induce Hsp70 and Hsp27 in SH-SY5Y human neuroblastoma cells. Both compounds were extremely potent at inducing Hsp70 and Hsp27 and were found to be effective inducers in the nanomolar range (Fig. 5c). Expansion of the dose–response curves to low nanomolar doses demonstrated that geldanamycin was more potent than 19-phenyl geldanamycin at Hsp induction (Supplementary Fig. S16), but, importantly, both geldanamycin and 19-phenyl geldanamycin were more potent at the induction of Hsp70 and Hsp27 than 17-AAG, the benzoquinone ansamycin that advanced to Phase II clinical trial (Fig. 5c). The effect of 19-substituted benzoquinone ansamycins on both oncogenic client proteins in tumour cells and their ability to induce a compensatory increase in Hsp70 and Hsp27 levels in dopaminergic cells, particularly when coupled with their lower toxicity to normal cells, suggests that these novel compounds may have useful therapeutic applications.

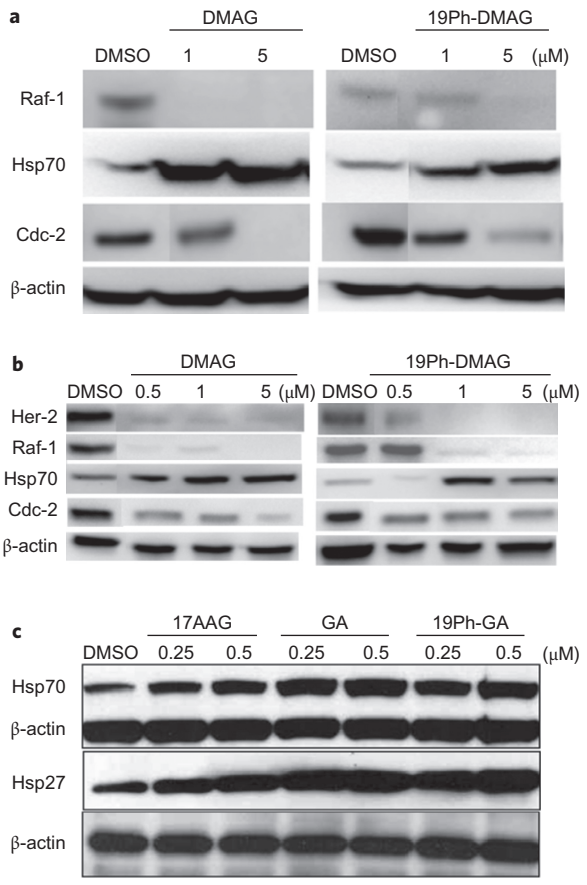

Figure 5 | Evaluation of 19-substituted compounds as inhibitors of Hsp90 in cellular systems. a, Immunoblot analysis of biomarkers of Hsp90 inhibition in MDA468-NQ16 human breast cancer cells treated with either 17-DMAG or 19-phenyl 17-DMAG for 48 h and immunoblotted for the Hsp90 clients Raf-1, Cdc-2 and for Hsp70. **b**, Immunoblot analysis of biomarkers of Hsp90 inhibition in BT474 human breast cancer cells treated with either 17-DMAG or 19-phenyl 17-DMAG for 48 h and immunoblotted for the Hsp90 clients Her-2 Raf-1, Cdc-2 and for Hsp70. **c**, Immunoblot analysis of Hsp70 and Hsp27 induction in SH-SY5Y neuroblastoma cells following treatment with either 17-AAG, geldanamycin or 19-phenyl geldanamycin for 16 h. In general, we observe a decrease in Hsp90 client proteins (Raf-1, Her-2 and Cdc-2) and a compensatory increase in other Hsps (27 and 70), the two most common biomarkers used for inhibition of Hsp90 in cells. Results are representative of three separate experiments. β-actin was used as a loading control.

In this study, the power of palladium-catalysed coupling reactions has been demonstrated with the synthesis of a range of novel 19-substituted benzoquinone ansamycins, specifically designed to both block nucleophilic attack at C19, a potential source of metabolic instability and toxicity, and to cause a conformational switch to facilitate protein binding. NMR spectroscopy established that the resulting macrocycles did indeed adopt the desired *cis*-amide conformation, while protein X-ray crystallography showed that the compounds bound to the *N*-terminal ATP site of Hsp90. Importantly, the 19-substituted benzoquinone ansamycins were found to be markedly less toxic to normal endothelial and epithelial cell systems than their parent quinones. Studies in both human cancer cells and dopaminergic neural cells established that the 19-substituted benzoquinone ansamycins are effective inhibitors of Hsp90, exhibiting the appropriate molecular signature: decreases

in Hsp90 client proteins and a compensatory increase in other heat shock proteins including Hsp70 and Hsp27. When considered together with their markedly decreased toxicity to normal cells, this suggests that 19-substituted benzoquinone ansamycins may have a greater therapeutic window than their parent quinones and hence considerable potential for application in the therapy of cancer and neurodegenerative diseases.

Methods

All experimental procedures, characterization data for all compounds and copies of the ^{1}H and ^{13}C NMR spectra, details of NMR studies, biological evaluations and protein crystallography are given in the Supplementary Information.

Received 8 November 2012; accepted 4 February 2013; published online 10 March 2013

References

1. McDonald, E., Workman, P. & Jones, K. Inhibitors of the Hsp90 molecular chaperone: attacking the master regulator in cancer. *Curr. Top. Med. Chem.* **6,** 1091–1107 (2006).
2. Janin, Y. L. ATPase inhibitors of heat-shock protein 90, second season. *Drug Discov. Today* **15,** 342–353 (2010).
3. Porter, J. R., Fritz, C. C. & Depew, K. M. Discovery and development of Hsp90 inhibitors: a promising pathway for cancer therapy. *Curr. Opin. Chem. Biol.* **14,** 412–420 (2010).
4. Fadden, P. *et al.* Application of chemoproteomics to drug discovery: identification of a clinical candidate targeting Hsp90. *Chem. Biol.* **17,** 686–694 (2010).
5. Massey, A. J. ATPases as drug targets: insights from heat shock proteins 70 and 90. *J. Med. Chem.* **53,** 7280–7286 (2010).
6. Trepel, J., Mollapour, M., Giaccone, G. & Neckers, L. Targeting the dynamic Hsp90 complex in cancer. *Nature Rev. Cancer* **10,** 537–549 (2010).
7. Biamonte, M. A. *et al.* Heat shock protein 90: inhibitors in clinical trials. *J. Med. Chem.* **53,** 3–17 (2010).
8. Gallo, K. A. Targeting Hsp90 to halt neurodegeneration. *Chem. Biol.* **13,** 115–116 (2006).
9. Waza, M. *et al.* Modulation of Hsp90 function in neurodegenerative disorders: a molecular-targeted therapy against disease-causing protein. *J. Mol. Med.* **84,** 635–646 (2006).
10. Luo, G-R., Chen, S. & Le, W-D. Are heat shock proteins therapeutic target for Parkinson's disease? *Int. J. Biol. Sci.* **3,** 20–26 (2007).
11. Adachi, H. *et al.* Heat shock proteins in neurodegenerative diseases: pathogenic roles and therapeutic implications. *Int. J. Hyperther.* **25,** 647–654 (2009).
12. Sajjad, M. U., Samson, B. & Wyttenbach, A. Heat shock proteins: therapeutic drug targets for chronic neurodegeneration? *Curr. Pharm. Biotechnol.* **11,** 198–215 (2010).
13. Kalia, S. K., Kalia, L. V. & McLean, P. J. Molecular chaperones as rational drug targets for Parkinson's disease therapeutics. *CNS Neurol. Disord.: Drug Targets* **9,** 741–753 (2010).
14. Aridon, P. *et al.* Protective role of heat shock proteins in Parkinson's disease. *Neurodegen. Dis.* **8,** 155–168 (2011).
15. Supko, J. G., Hickman, R. L., Grever, M. R. & Malspeis, L. Preclinical pharmacological evaluation of geldanamycin as an antitumor agent. *Cancer Chemother. Pharmacol.* **36,** 305–315 (1995).
16. Cysyk, R. L. *et al.* Reaction of geldanamycin and C17-substituted analogues with glutathione: product identifications and pharmacological implications. *Chem. Res. Toxicol.* **19,** 376–381 (2006).
17. Lang, W. *et al.* Biotransformation of geldanamycin and 17-allylamino-17-demethoxygeldanamycin by human liver microsomes: reductive versus oxidative metabolism and implications. *Drug Metab. Dispos.* **35,** 21–29 (2007).
18. Guo, W., Reigan, P., Siegel, D. & Ross, D. Enzymatic reduction and glutathione conjugation of benzoquinone ansamycin heat shock protein 90 inhibitors: relevance for toxicity and mechanism of action. *Drug Metab. Dispos.* **36,** 2050–2057 (2008).
19. Stebbins, C. E. *et al.* Crystal structure of an Hsp90–geldanamycin complex: targeting of a protein chaperone by an antitumor agent. *Cell* **89,** 239–250 (1997).
20. Roe, S. M. *et al.* Structural basis for inhibition of the Hsp90 molecular chaperone by the antitumor antibiotics radicicol and geldanamycin. *J. Med. Chem.* **42,** 260–266 (1999).
21. Dehner, A. *et al.* NMR chemical shift perturbation study of the N-terminal domain of Hsp90 upon binding of ADR AMP-PNP, geldanamycin, and radicicol. *ChemBioChem* **4,** 870–877 (2003).
22. Modi, S. *et al.* HSP90 inhibition is effective in breast cancer: a phase 2 trial of tanespimycin (17AAG) plus trastuzumab in patients with HER2-positive metastatic breast cancer progressing on trastuzumab. *Clin. Cancer Res.* **17,** 5132–5139 (2011).
23. Shen, H-Y. *et al.* Geldanamycin induces heat shock protein 70 and protects against MPTP-induced dopaminergic neurotoxicity in mice. *J. Biol. Chem.* **280,** 39962–39969 (2005).
24. Waza, M. *et al.* 17-AAG, an Hsp90 inhibitor, ameliorates polyglutamine-mediated motor neuron degeneration. *Nature Med.* **11,** 1088–1095 (2005).
25. Waza, M. *et al.* Alleviating neurodegeneration by an anticancer agent—an Hsp90 inhibitor (17-AAG). *Ann. NY Acad. Sci.* **1086,** 21–34 (2006).
26. Tadtong, S. *et al.* Geldanamycin derivatives and neuroprotective effect on cultured P19-derived neurons. *Bioorg. Med. Chem. Lett.* **17,** 2939–2943 (2007).
27. Rinehart, K. L. & Shield, L. S. Chemistry of the ansamycin antibiotics. *Prog. Chem. Org. Nat. Prod.* **33,** 231–307 (1976).
28. Schnur, R. C. & Corman, M. L. Tandem [3,3]-sigmatropic rearrangements in an ansamycin—stereospecific conversion of an (S)-allylic alcohol to an (S)-allylic amine derivative. *J. Org. Chem.* **59,** 2581–2584 (1994).
29. Jez, J. M. *et al.* Crystal structure and molecular modeling of 17-DMAG in complex with human Hsp90. *Chem. Biol.* **10,** 361–368 (2003).
30. Lee, Y-S., Marcu, M. G. & Neckers, L. Quantum chemical calculations and mutational analysis suggest heat shock protein 90 catalyzes *trans–cis* isomerization of geldanamycin. *Chem. Biol.* **11,** 991–998 (2004).
31. Thepchatri, P. *et al.* Relationship among ligand conformations in solution, in the solid state, and at the Hsp90 binding site: geldanamycin and radicicol. *J. Am. Chem. Soc.* **129,** 3127–3134 (2007).
32. Onuoha, S. C. *et al.* Mechanistic studies on Hsp90 inhibition by ansamycin derivatives. *J. Mol. Biol.* **372,** 287–297 (2007).
33. Reigan, P., Siegel, D., Guo, W. & Ross, D. A mechanistic and structural analysis of the inhibition of the 90-kDa heat shock protein by the benzoquinone and hydroquinone ansamycins. *Mol. Pharmacol.* **79,** 823–832 (2011).
34. Janin, Y. L. Heat shock protein 90 inhibitors. A text book example of medicinal chemistry. *J. Med. Chem.* **48,** 7503–7512 (2005).
35. Wrona, I. E., Agouridas, V. & Panek, J. S. Design and synthesis of ansamycin antibiotics. *C. R. Chimie* **11,** 1483–1522 (2008).
36. Sasaki, K. & Inoue, Y. Geldanamycinderivate und Antitumormittel mit einem Gehalt derselben. German patent 3,006,097 (1980).
37. Schnur, R. C. *et al.* Inhibition of the oncogene product P185(Erbb-2) *in vitro* and *in vivo* by geldanamycin and dihydrogeldanamycin derivatives. *J. Med. Chem.* **38,** 3806–3812 (1995).
38. Rinehart, K. L. *et al.* Synthesis of hydrazones and oximes of geldanaldehyde as potential polymerase inhibitors. *Bioorg. Chem.* **6,** 341–351 (1977).
39. Sasaki, K. & Inoue, Y. Novel geldanamycin derivatives as pharmaceutically active ingredients and their preparation. Japan patent JP 57-163369 (1981).
40. Wu, L. *et al.* Geldanamycin biosynthetic analog 19-O-glycylgeldanamycin. China patent CN 101792418A (2010).
41. Farina, V. & Krishnan, B. Large rate accelerations in the Stille reaction with tri-2-furylphosphine and triphenylarsine as palladium ligands—mechanistic and synthetic implications. *J. Am. Chem. Soc.* **113,** 9585–9595 (1991).
42. Negishi, E-I. *et al.* Nickel-catalyzed or palladium-catalyzed cross coupling. 31. Palladium-catalyzed or nickel-catalyzed reactions of alkenylmetals with unsaturated organic halides as a selective route to arylated alkenes and conjugated dienes—scope, limitations, and mechanism. *J. Am. Chem. Soc.* **109,** 2393–2401 (1987).
43. Liebeskind, L. S. & Fengl, R. W. 3-Stannylcyclobutenediones as nucleophilic cyclobutenedione equivalents—synthesis of substituted cyclobutenediones and cyclobutenedione monoacetals and the beneficial effect of catalytic copper iodide on the Stille reaction. *J. Org. Chem.* **55,** 5359–5364 (1990).
44. Harrowven, D. C. *et al.* Potassium carbonate–silica: a highly effective stationary phase for the chromatographic removal of organotin impurities. *Chem. Commun.* **46,** 6335–6337 (2010).
45. Guo, W. *et al.* Formation of 17-allylamino-demethoxygeldanamycin (17-AAG) hydroquinone by NAD(P)H:quinone oxidoreductase 1 (NQO1): role of 17-AAG hydroquinone in heat shock protein 90 inhibition. *Cancer Res.* **65,** 10006–10015 (2005).
46. Guo, W. *et al.* The bioreduction of a series of benzoquinone ansamycins by NAD(P)H: quinone oxidoreductase 1 to more potent heat shock protein 90 inhibitors, the hydroquinone ansamycins. *Mol. Pharmacol.* **70,** 1194–1203 (2006).
47. Siegel, D. *et al.* Role for NAD(P)H:quinone oxidoreductase 1 and manganese-dependent superoxide dismutase in 17-(allylamino)-17-demethoxygeldanamycin-induced heat shock protein 90 inhibition in pancreatic cancer cells. *J. Pharmacol. Exp. Ther.* **336,** 874–880 (2011).
48. Kitamura, Y. *et al.* Protective effects of the anti-Parkinsonian drugs talipexole and pramipexole against 1-methyl-4-phenylpyridinium-induced apoptotic death in human neuroblastoma SH-SY5Y cells. *Mol. Pharmacol.* **54,** 1046–1054 (1998).
49. Smith, W. W. *et al.* alpha-Synuclein phosphorylation enhances eosinophilic cytoplasmic inclusion formation in SH-SY5Y cells. *J. Neurosci.* **25,** 5544–5552 (2005).
50. Jeong, H. J. *et al.* Transduced Tat-DJ-1 protein protects against oxidative stress-induced SH-SY5Y cell death and Parkinson disease in a mouse model. *Mol. Cell* **33,** 471–478 (2012).

Acknowledgements

The authors acknowledge support from the Parkinson's Disease Society UK (R.R.A.K. and C.J.M.). The work was also supported by the National Institutes of Health (NIH grants CA51210 and ES018943; D.R., D.S., C-H.C. and R.X.). The authors thank S. Aslam and K. Butler for help with NMR studies, and S. Young (University of Nottingham, ICPMS), M. Cooper and G. Coxhill (University of Nottingham, mass spectrometry) for technical assistance.

Author contributions

D.R. and C.J.M. jointly conceived the project, and directed the biology and chemistry, respectively. R.R.A.K. was responsible for the design and execution of the chemistry. NMR studies and molecular modelling were carried out by R.R.A.K., H.E.L.W. and A.L.D., and W.L. carried out small-molecule X-ray crystallography. The biological studies were co-directed by D.S., and carried out by C-H.C., D.L.D. and R.X. Protein crystallography was directed by C.P. and carried out by C.P. and S.M.R. All authors contributed to the preparation of the manuscript.

Additional information

Supplementary information and chemical compound information are available in the online version of the paper. Reprints and permissions information is available online at www.nature.com/reprints. Correspondence and requests for materials should be addressed to C.P., D.R. and C.J.M.

Competing financial interests

The authors declare no competing financial interests.